Atom Indonesia

Journal homepage: http://atomindonesia.brin.go.id

The Impact of Different Light-Reflecting Materials Compositions of ($LaBr_3$:Ce) Scintillation Detector on Spent Nuclear Fuel Gamma Spectrum

R. A. El-Tayebany

Nuclear and Radiological Safety Research Center, Egyptian Atomic Energy Authority, Cairo, Egypt

ARTICLE INFO

Article history:
Received 15 January 2024
Received in revised form 4 March 2024
Accepted 30 March 2024

Keywords:

MCNPX, $LaBr_3$(Ce) scintillators
Absolute efficiency
Light-reflecting materials
Gamma-ray

ABSTRACT

The Scintillation detectors are extensively employed in nuclear safeguards, nuclear security fields, radioactive material testing, and physics research. Light-reflecting materials of ($LaBr_3$:Ce) scintillation detectors positively affect their ability to capture light. Our goal is to investigate the characteristics of various reflectors by MCNPX code. In this paper, high-activity fission products from the spent fuel, identified as the utilized radionuclides ^{152}Eu, ^{154}Eu ^{134}Cs, ^{137}Cs, and ^{243}Cm, have been used in the simulation. Also, short-lived fission products, and short-lived actinides (^{239}U and ^{239}Np), which have decay heat in the timeframe of severe accident analysis, have been included. The findings of this investigation are consistent with the discovery that $LaBr_3$:Ce delivers superior resolution. Additionally, some closely spaced peaks in the spectra of numerous radioisotopes could be resolved by the $LaBr_3$:Ce detector. With different energy lines, the spectral responses of the scintillators' various reflectors were evaluated.

INTRODUCTION

Characterizing spent nuclear fuel presents a variety of challenges for single-detector gamma spectroscopy. The following three issues are addressed by this system: high count rates restrict data collection rates and lower statistical precision.

Field research frequently makes use of handheld, portable gamma-ray spectrometers. Portable threshold spectrometers use several switch-operated energy thresholds and up to 100 cm3 of NaI(Tl) crystals as detectors. Interfering and powerful peak detection are complicated by Compton scattering in gamma spectra from a range of fission products, and the transportation of spent nuclear fuel is costly and time-consuming because of challenges with safety and regulations. Compared to sodium iodide thallium-doped (NaI: Tl), $LaBr_3$:Ce is more efficient. It has been demonstrated that for a 1.5" by 1.5" detector over 350 keV, $LaBr_3$:Ce performs 1.2-1.65 times higher than NaI: Tl detectors. $LaBr_3$:Ce also has a higher energy resolution than NaI: Tl. $LaBr_3$:Ce displays an energy resolution of 2.5-3 % at the 662 keV gamma-line of ^{137}Cs as opposed to NaI: Tl' 6-7 %. [1-3]. Some research indicates that $LaBr_3$:Ce detects more peaks and does so with greater efficiency than NaI: Tl. This demonstrates the benefits of $LaBr_3$:Ce over NaI: Tl. $LaBr_3$:Ce systems are considerably more mobile than HPGe systems since nitrogen cooling is not required. LaBr3:Ce can function well at count rates up to 500 kHz and has proven to be a great detector option for high count rate settings [4,5].

The successful identification of isotopes in a fuel element spectrum by $LaBr_3$:Ce scintillators has been demonstrated using MCNPX simulations. These findings imply that $LaBr_3$:Ce will also help characterize spent nuclear fuel [6,7]. However, the application of $LaBr_3$:Ce application has certain limitations. First, it is impossible to create a pure crystal of $LaBr_3$:Ce due to the abundant natural lanthanum and its isotopic impurities of ^{138}La. It is clear from this that there is internal ^{138}La radioactivity, which produces an intrinsic background spectrum specific to this sort of detector. This internal radioactivity is primarily caused by the tiny

*Corresponding author.
E-mail address: rreltyebany@gmail.com
DOI:

contaminants ^{138}La and ^{227}Ac in the scintillator. About 0.09 % of lanthanum found in nature is made of ^{138}La. It emits 2 gamma-rays: 1 at 1435.8 keV from electron capture to ^{138}Ba and one at 788.7 keV from beta decay to ^{138}Ce. The half-life of ^{138}La is 1.06×10^{11} years, which explains why these activity levels, measured at 0.065 and 0.068 cps cm^{-3}, respectively, are relatively low [8].

The Monte Carlo approach is the most dependable way to determine the specific properties of light collection in scintillation detectors. However, the ability to make basic approximations is also important, particularly during the detector design phase. As far as we know, there haven't been any systematic studies on this issue. We refer to both the Monte Carlo simulations and their intercomparison with the data and models. These computations were used to examine how various reflectors affected the plastic detectors' capacity to capture light [9]. Some researchers Used the Monte-Carlo codes "PHOTON" and "LIGHT," to examine the process of light gathering in a scintillation counter with a diffuse reflector. The resulting observations are compared with the simple model estimations and used to reanalyze the prior NE-2 13 transparency measurements and explain the time structure of the signal for many detectors, including the full absorption neutron spectrometer. Another research team worked on creating materials that reflect light and are utilized in pixelated scintillator detectors. For the first time, a low-cost DLP 3D printing process was used to generate the reflecting surfaces for pixels ranging in size from 0.8 to 3.2 mm. The composite of transparent ultraviolet light-cured resin and TiO_2 as a light-scattering filler was used as the material for the reflectors. It was noted that TiO_2 performed better than other pigments like $BaSO_4$, hBN, or cubic zirconia [10]. In a different research study, the attenuation characteristics of photons from Ce-doped $Gd_3Al_2Ga_3O_{12}$ (Ce: GAGG) scintillators were examined by testing samples of different sizes. They discussed the factors that cause the reduction of light scintillation. The self-absorption of the Ce: GAGG scintillator is the primary factor, while geometrical effects such as the reflecting capabilities of the reflector wrapping are secondary [11].

Our research aims to enhance the ($LaBr_3$:Ce) scintillation detector's performance by altering the detector's light-reflecting materials and observing the impact on the gamma spectrum of important isotopes produced by spent nuclear fuel measurement.

MATERIALS AND METHODS

$LaBr_3$(Ce) detector simulation

A scintillation element reflector is one of the crucial components of a scintillation detector. In theory, a photodetector attached to the scintillator from one side should be able to capture all of the light emitted inside a material during a scintillation process. To guide as much of the generated light towards the photodetector as possible, the scintillator's reflecting coating is required. Therefore, the reflector's characteristics have a substantial impact on how much light is gathered from the utilized scintillator, which can dramatically enhance the detector's final performance. Teflon tape is used frequently in scintillation measurements and is regarded as a standard wrapping [12,13].

Lanthanum bromide ($LaBr_3$) is a quick and effective scintillation crystal when activated with a small amount of cerium. Due to its extremely high light output across a wide temperature range, quick time response, and resulting energy resolution capability, the $LaBr_3$:Ce scintillator is highly attractive and may be applied to practically all nuclear radiation detection sectors. The real and simulated $LaBr_3$:Ce 2” × 2” are shown in Figs. (1,2), respectively. The materials used in the simulations are the crystal material ($LaBr_3$) with a density of 5.09 g/cm^3, the dry air with a density of 0.00122 g/cm^3, Al-housing with a density of 2.7 g/cm^3, and rubber cover with a density 0.92 g/cm^3. Additionally, the setup simulation was carried out using various cards involved in the input file of MCNPX. These cards include the cell card, surface card, data card, and tally card. All these cards contain the geometries of the detector, the source location, information on the radioactive sources used such as the energy lines that are selected (see Table 2), and the source position. In our case, the source is placed close to the detector.

Fig. 1. $LaBr_3$:Ce Crystals.

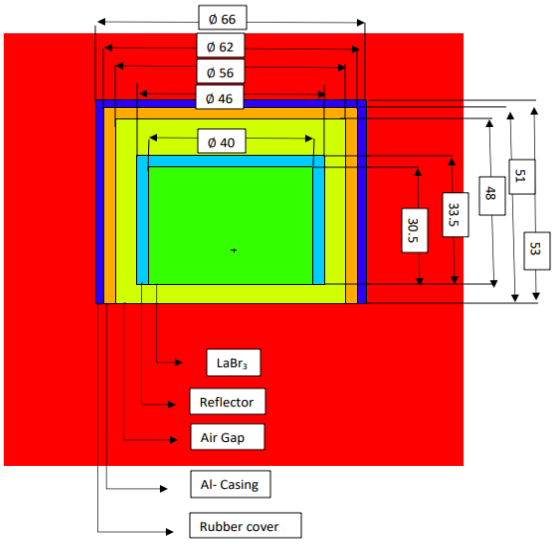

Fig. 2. Model of the $LaBr_3$(Ce) detector in MCNP6 (All the dimensions in mm).

Light-reflecting materials

Reflectivity, or ρ, is defined as the proportion of the radiation flux (μ_r) reflected by material to the incident radiation flux (μ_i) as written in Eq. (1)

$$\rho = \mu_r / \mu_i \quad (1)$$

If the refractive index (n) and absorption index (χ) of the sample material are known, the reflectivity value as a function of an incident angle can be computed using Fresnel's formulas.

The following formulas in Eqs. (2,3) are used for the perpendicular (⊥) and parallel (||) components of incoming radiation that are polarized in two neighboring media (1 and 2), where the absorption indices (x1 and x2) are minimal relative to the refractive indices (n1 and n2).

$$\rho_{\perp} = \left(\frac{\cos\varphi - \sqrt{n_{21}^2 - sin^2\,\varphi}}{\cos\varphi + \sqrt{n_{21}^2 - sin^2\,\varphi}} \right)^2 \quad (2)$$

$$\rho_{\parallel} = \left(\frac{n_{21}^2 \cos\varphi - \sqrt{n_{21}^2 - sin^2\,\varphi}}{n_{21}^2 \cos\varphi + \sqrt{n_{21}^2 - sin^2\,\varphi}} \right)^2 \quad (3)$$

where φ is the incidence radiation angle from the first medium onto the second concerning the surface normal, and $n_{21} = n_2/n_1$ [8].

The incident natural unpolarized radiation's perpendicular and parallel components have identical intensities, and reflectivity can be determined by taking the radiation's mean mathematical value as in Eq. (4)

$$\rho = \frac{1}{2}(\rho_{\perp} + \rho_{\parallel}) \quad (4)$$

In simulation, we used different types of reflectors, with different densities as shown in Table 1. The components and materials of the $LaBr_3$(Ce) detector include a Teflon reflector which is considered the default as shown in Fig. 3. These materials were selected because they are common reflectors for scintillation detectors and have high capabilities to reflect a large number of optical photons.

Table 1. The modeled light-reflecting materials in $LaBr_3$:Ce.

Reflectors	Density (g/cm^3)
Teflon (Default)	2.20
Al Mylar	1.39
TiO_2	4.23
Al-foil tap	2.70

Fig. 3. Default reflectors for LaBr3:Ce (Teflon).

RESULTS AND DISCUSSION

Conventional techniques for this confirmation rely on non-destructive (NDA) gamma-ray spectroscopy with sodium iodide (NaI) or high-purity germanium (HPGe) detectors [2]. HPGe is typically chosen when measurement conditions are unfavorable, such as high background levels, constrained measurement time, or low enrichment. Recently, detectors for Lanthanum Bromide ($LaBr_3$) have entered the commercial market. This kind of detector is expected to significantly increase the performance of NDA-based methods, which are frequently employed for ^{235}U enrichment determination, based on the technical information provided by suppliers. To appropriately analyze gamma-ray spectra produced with this new

type of detector, it is also anticipated that new algorithms for gamma-ray analysis will be created [14,15].

One method often used to characterize radioactive materials is gamma-ray spectroscopy. Atoms that are undergoing radioactivedecay release gamma and x-rays that are specific to the radioactive isotope. These spectral lines are employed in applications involving spent fuel to confirm the existence of fission product actinides. To provide a qualitative assessment of the spent fuel burnup, absolute activity measurements of ^{137}Cs can be carried out on spent fuel rods and assemblies; however, this needs the assembly attenuation and measurement geometry to be known or properly computed. Further computation can then determine the fissile mass content. The proportion of activities for particular isotopes of fission products can also be used to determine the burnup of wasted fuel. With burnup, the ratio of ^{134}Cs to ^{137}Cs is almost linear; however, for long-burned fuels, isotope decay must be taken into account. Gamma-ray attenuation in assemblies necessitates an additional correction to the gamma activity ratio approach. For field measurements, fission product activity ratios are simpler to calculate than absolute activities because all that is needed to know is the ratio of the detector efficiencies, which depend on the gamma-ray energy. Canisters or casks containing used fuels are probably not suitable for these approaches due to attenuation effects [16].

In this work, the selected gamma energy lines which added to the input file of the Monte Carlo code are shown in Table 2.

Table 2. The significant energy lines for different sources.

The Used Source	Significant Gamma Energy Lines (keV)
^{137}Cs	661.7
^{134}Cs	604.7
^{243}Cm	277.6
^{152}Eu	1408
^{154}Eu	1230.7
^{239}Np	106.13
^{239}U	74.66

By calculating the reflectivity of the reflectors using ^{137}Cs as shown in Fig. 4, we found that the TiO_2 and Al-foil reflectors give greater response at low energy compated to the others, but give the same effect in the rest of the energy range. Also, the significant energy range of ^{137}Cs (580-650 keV), which is maximized as shown in Fig. 5, has nearly the same reflectivity values.

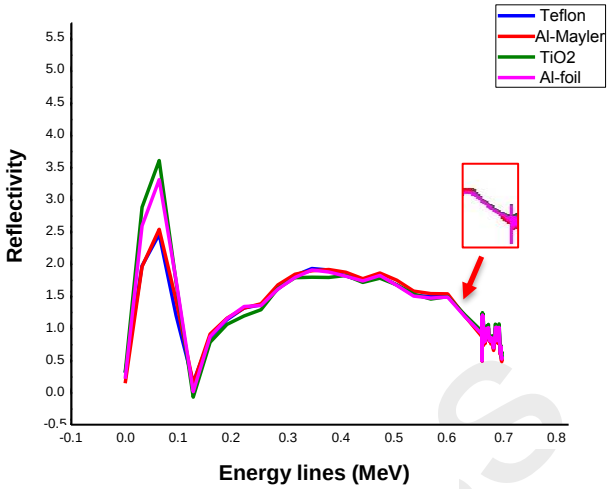

Fig. 4. Reflectivity using different reflectors for ^{137}Cs.

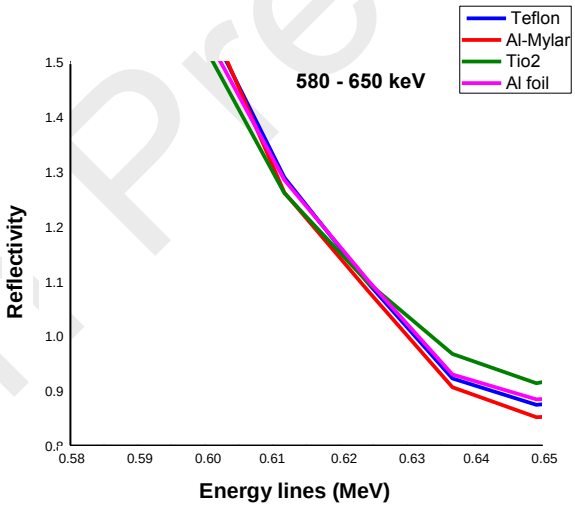

Fig. 5. The significant region (580-650 keV) for ^{137}Cs.

The same calculations are applied using different radioactive elements, as shown in Fig. 6, at different significant energy ranges which include energy lines with the highest branching ratio. We notice that all the curves show that Al-Mylar has the highest reflectivity values across the significant energy range. That's because the radiation flux (μ_r) reflected by the material to the incident radiation flux (μ_i) is large concerning the other reflecting materials. It depends on the refractive and absorption indices of the Al-Mylar.

The difference between the reflectivity value of the simulated reflectors R_n to the default one (Teflon) R_d is shown in Fig. 7, where, the bars denote that (R_n - R_d). Al-Mylar shows the highest reflectivity values across the significant energy range, as illustrated in Fig. 7. The negative values indicate that the reflectivity values are less than those obtained from the default reflector (Teflon) and vice versa in the positive values.

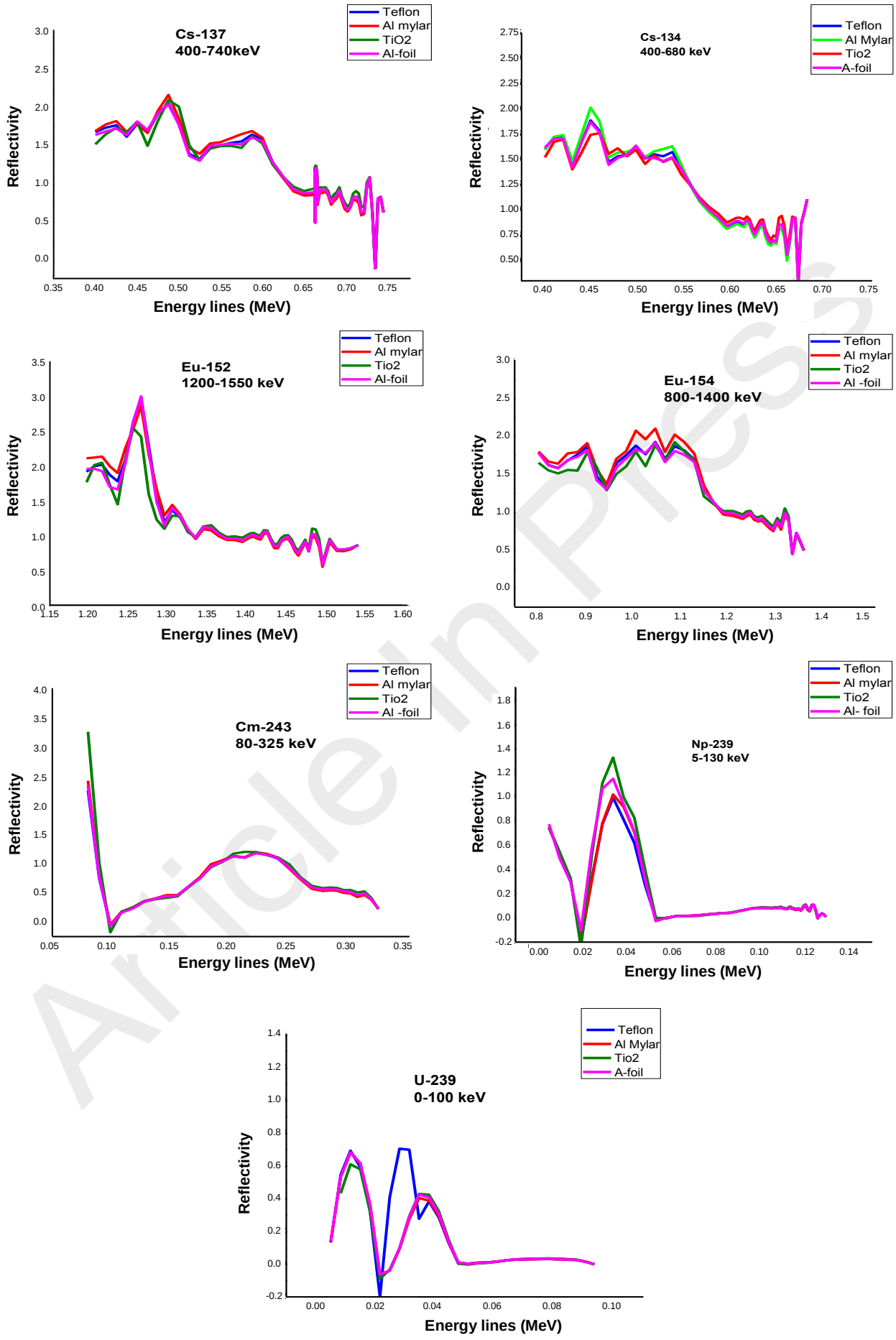

Fig. 6. Reflectivity at significant regions for different isotopes.

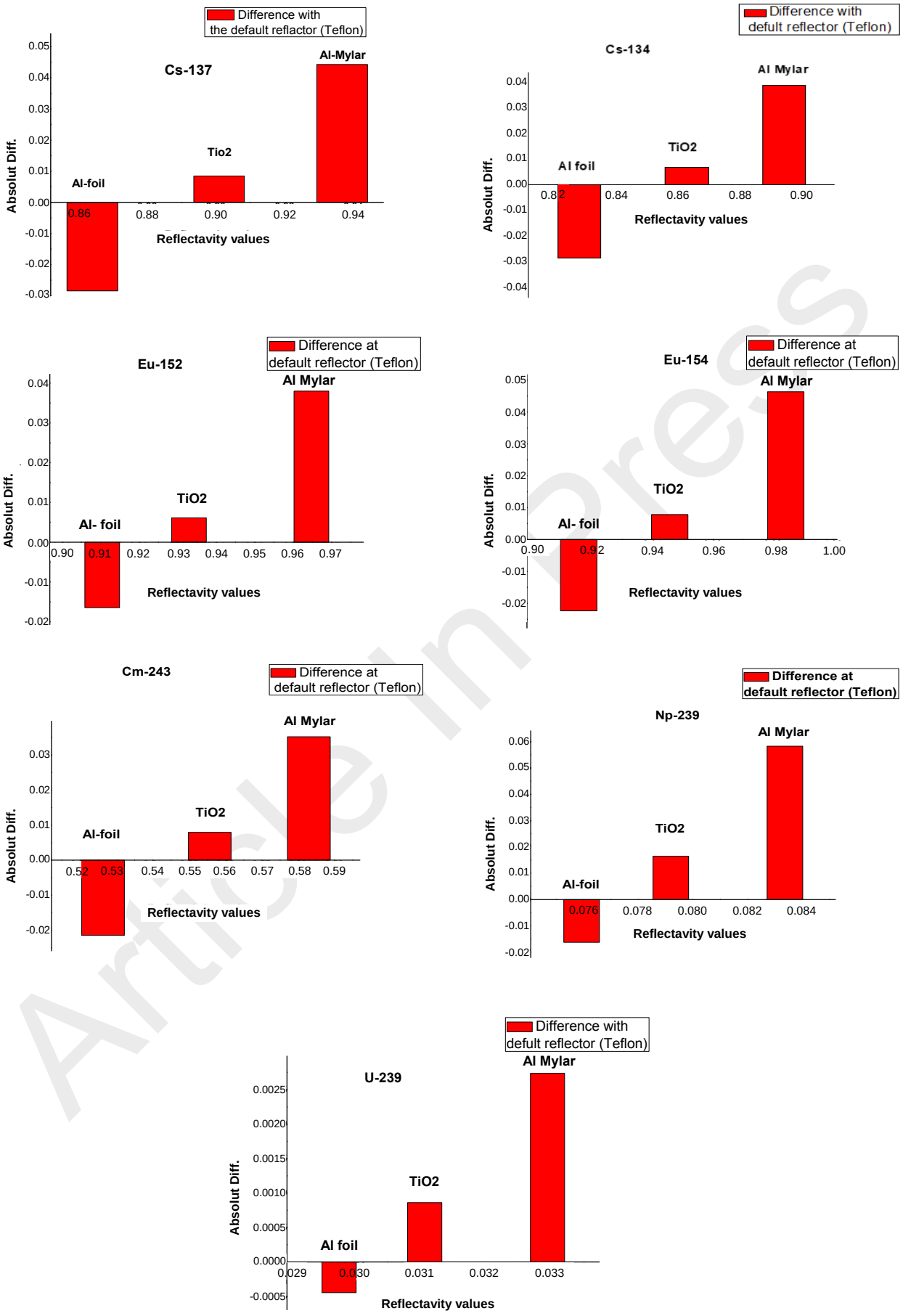

Fig. 7. The absolute difference values with the default reflector (Teflon) for the simulated isotopes.

CONCLUSION

A plastic scintillator with a rod shape had spectral output investigated, as well as the impact of the type of reflector and its application. The results showed that the detector output significantly depends on the reflecting material. The findings demonstrated that the best choice for reflectors' external wrapping had an impact on the detector's performance, observed across various types of fission products for spent fuel (^{152}Eu,^{154}Eu ^{134}Cs,^{137}Cs, Cm^{243}, ^{239}U, and ^{239}Np). The results demonstrated that the Al-Mylar reflector showed the largest absolute difference compared to the Teflon reflector. Also, it proved a good indication for the maximum reflectivity values across the significant energy range. Consequently, this positively affects the increase in counts for selected peaks and enhances the efficiency of the ($LaBr_3$:Ce) detector.

ACKNOWLEDGMENT

The author would like to thank the Egyptian Atomic Energy Authority and the Nuclear and Radiological Safety Research Center for their support and motivation.

AUTHOR CONTRIBUTION

R. A. El-Tayebany contributed as the main contributor to this paper.

REFERENCES

1. H. Syaeful, I.G. Sukadana *et al.*, Atom Indones. **40** (2014) 33.
2. S. G. Crystal, Scintillation Products Technical Note: BrilLanCe™ Scintillators Performance Summary, Saint-Gobain Crystal, Ohio (2016).
3. K. Ciupek, S. Jednoróg, M. Fujak *et al.*, J. Radioanal. Nucl. Chem. **299** (2014) 1345.
4. B. D Milbrath, B. J. Choate, J. E. Fast *et al.*, Nucl. Instrum. Methods Phys. Res., Sect. A, **572** (2007) 774.
5. B. Löher, D. Savran, E. Fiori *et al.*, Nucl. Instrum. Methods Phys. Res., Sect. A, **686** (2012) 1.
6. A. Dreschera , M. Yohoa, S. Landsbergera *et al.*, *Development of $LaBr_3$:Ce Scintillation Detectors for a Gamma-Gamma Coincidence System with Applications in Spent Nuclear Fuel*, The University of Texas at Austin Nuclear Engineering Teaching Laboratory Pickle Research Campus R-9000 Austin, TX 78712, USA (2016).
7. J. Navarro, T. A. Ring and D. W. Nigg, Nucl. Data Sheets **118** (2014) 571.
8. A. Y. Vorob'ev, V. A. Petrov, V. E. Titov *et al.*, Thermophysical Properties of Materials, **45** (2007) 19.
9. V. A. Baranov, V. V. Filchenkov, A. D. Konin *et al*., Nucl. Instrum. Methods Phys. Res., Sect. A, **374** (1996) 335.
10. P. S. Sokolov, D. A. Komissarenko, S. K. Belus *et al.*, Opt. Mater. **108** (2020) 110393.
11. N. Uchida, H. Takahashi, M. Ohno *et al.*, Nucl. Instrum. Methods Phys. Res., Sect. A, **986** (2021) 164725.
12. M. Janecek and W. W. Moses, IEEE Trans. Nucl. Sci. **55** (2008) 2432.
13. L. Stuhl, A. Krasznahorkay, M. Csatlós *et al.*, J. Phys. Conf. Ser. **665** (2016) 012050.
14. F. C Dias, M. S. Grund, G. Renha Jr. *et al*., *The Use of Lanthanum Bromide Detectors for Nuclear Safeguards Applications*, International Nuclear Atlantic Conference (2009).
15. D. Reily, N. Ensslin, H. Jr. Smith *et al*., *Passive Nondestructive Assay of Nuclear Materials*, NUREG/CR-5550, US-NRC (1991).
16. M. Tarvainen, F. Levai, T. E. Valintine *et al*., *NDA Techniques for Spent Fuel Verification And Radiation Monitoring*, Report on Activities 6a and 6b of Task JNT C799 (SAGOR) Finnish Support Programme to the IAEA Safeguards, STUK-YTO-TR-133 (1997).